SECOND EUROPEAN CONFERENCE ON EARTHQUAKE ENGINEERING
AND SEISMOLOGY, ISTANBUL AUG. 25-29, 2014

ASSESSMENT OF THE SEISMIC RESPONSE OF A BASE ISOLATED HV CIRCUIT BREAKER WITH STEEL CABLE DAMPERS

Silvia ALESSANDRI[1], Renato GIANNINI[2], Fabrizio PAOLACCI[3], Marilena AMORETTI[4], Andrea FREDDO[5]

ABSTRACT

This paper briefly describes the design and the characterization of a new base isolation system for the seismic protection of HV ceramics circuit breakers, in order to be qualified according to the standard IEC 62271-207. The solution adopted is based on the use of steel cable dampers, already known as "Wire-Rope." Accurate numerical analyses and experimental tests performed on a typical HV breaker upon a shaking table demonstrated the effectiveness of the proposed solution. An on-site installation in several Italian substations of this system has permitted to verify the simplicity and rapidity of the intervention necessary for the seismic upgrading of the breaker.

INTRODUCTION

Substations are one of the most important parts in the electric power networks and play a vital role in the stability of electric transmission system. Yet the experiences gained from recent earthquakes in Italy (Emilia-Romagna 2012) have shown that some substation's components, especially the circuit breakers, are very vulnerable and the direct and indirect losses resulting from their damaging are sometimes really considerable and it can affect dramatically the overall system reliability. The seismic vulnerability of these apparatuses is due to their shape: they are slender and composed of brittle ceramic parts, with a large mass concentrated at the top.

In order to reduce the seismic vulnerability of HV apparatus and consequently of the entire national electric system, the Italian Transmission System Operator (TERNA) has established an agreement with the University Roma Tre to design a new base isolation system for the seismic protection of circuit breakers against seismic events of large intensity.

Seismic isolation devices, usually employed to protect buildings against earthquakes, are not suitable to protect HV electrical breakers. In fact, they are usually designed for horizontal shear forces, with a limited variation of vertical normal force and always in compression. This condition is practically impossible to be satisfied in case of extremely slender structures with mass lumped at the top, such as HV electrical breakers, because of the large overturning moment at the base. In this case, the increasing of period is due to the rocking of the base rather than its horizontal translation and the isolation devices could be subjected both to tension and compression. A similar device can be based on steel cable dampers (Wire-Ropes). They are very simple devices, consisting of a unique twisted stainless steel cable wound on drilled bars in aluminium alloy. The mechanical flexibility of the entire cable provides to the device optimal mechanical isolation properties in all three principal directions.

[1] Post Doc., University Roma Tre, Rome, Italy, silvia.alessandri@uniroma3.it
[2] Full Prof., University Roma Tre, Rome, Italy, renato.giannini@uniroma3.it
[3] Assisant Prof. University Roma Tre, Rome, Italy, fabrizio.paolacci@uniroma3.it
[3] Terna Rete Italia, Sviluppo Rete Ingegneria, Rome, Italy, marilena.amoretti@terna.it
[5] Terna Rete Italia, Sviluppo Rete Ingegneria, Rome, Italy, andrea.freddo@terna.it

They are often used for the vibrations control of industrial equipment (Schwanen, 2004), whereas they have never been adopted as seismic isolators, as demonstrated by theoretical studies only (Demetriades et al., 1993, Schwanen 2004, Paolacci and Giannini, 2008, Knight and Kempner, 2009, Kong and Rehinorn, 2009) and no practical applications. However, the use of Wire-Ropes for the base isolation of components of electric substations has been already considered in the past (Di Donna et al 2002). This paper illustrates the solution adopted for the isolation device and the analysis carried out to demonstrate its effectiveness.

ANALYTICAL MODEL OF THE CIRCUIT BREAKER

As a first step, the seismic vulnerability of a circuit breaker has been investigated. It is one of the poles of a circuit breaker for 420kV electric power networks, which is composed by two horizontal interruption chambers placed at the top of a support, consisting of two hollow ceramic columns connected each other and to the chambers by metallic joints. The lower column rests on a metallic box supported by an element made of two U200 steel girders, connected by stiffening brackets. Next to the chambers, there are two hollow ceramic elements, with function of capacitors. The metallic box under the ceramic columns houses the operating parts; laterally connected there is an operating cabinet containing an electric engine and others components to control the switch. In one of the three poles, another cabinet houses the electrical control panel. A scheme of the system in shown in Figure 1.

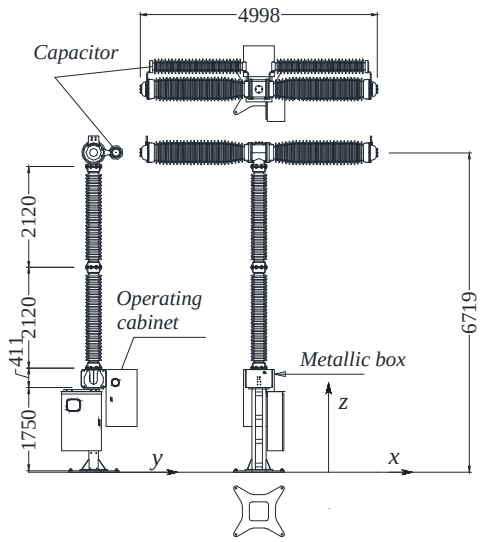

Figure 1. Arrangement of the circuit breaker

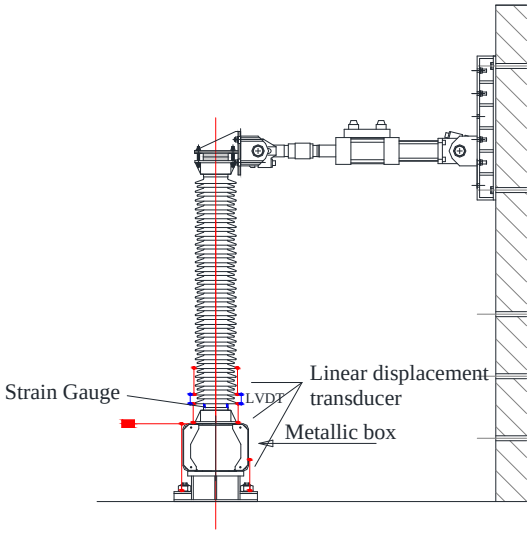

Figure 2. Test apparatus for the evaluation of the mechanical properties of the ceramic column and of the joints

The mechanical behaviour of the circuit breaker can be adequately described by an elastic model, because of the linear elastic behaviour of ceramic and because the columns are less strong than the steel support. Both, ceramic columns and steel frame, can be modelled by linear elastic beam elements. In order to assess the mechanical properties of ceramic columns (strength and elastic modulus), the connecting flanged joint and the supporting box, three experimental tests have been executed on different configurations: one with the column base connected to a rigid support, the others with the column base connected to the metallic box. The columns have been subjected to a cyclic quasi-static displacements history up to the column rupture. A sketch of the test apparatus is illustrated in Figure 2.

Figure 3(a) shows the experimental force-displacement cycle of one of the tests; it can been clearly seen that the behaviour is elastic until the collapse at the column base occurs (see Figure 3 (b)). The slight hysteretic behaviour is caused by the flanged joint deformability.

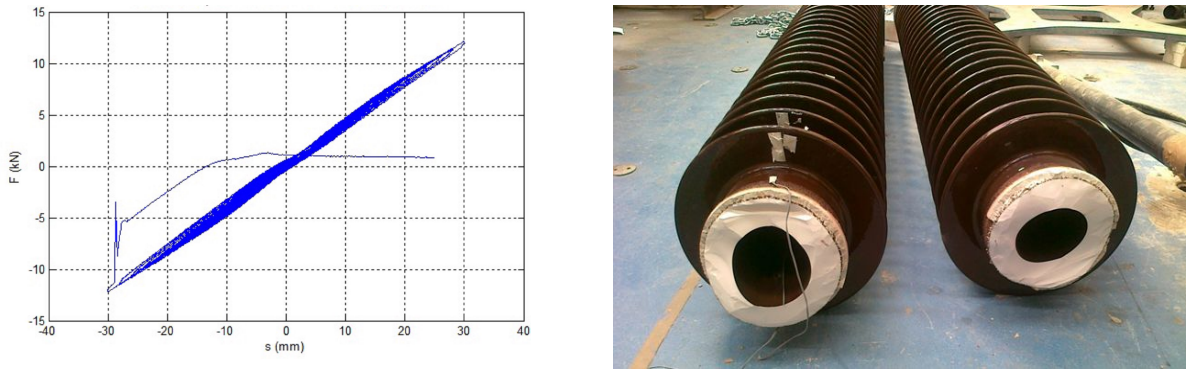

(a) (b)

Figure 3. Experimental force-displacement cycle (a) and rupture in the ceramic columns (b)

The experimental results have been compared with those obtained numerically by using the FE software Strand7 (Strand 7 Pty Ltd., 2010): an accurate finite element model has been developed by using brick elements for the column and the flanged joint, whereas shell elements have been used for the metallic box and the anchor system. The numerical results have been indirectly used to determine both the elastic modulus of ceramic and its ultimate stress; the ultimate moment of the column provided by all tests was identically equal to 25 kNm. Comparing displacements and rotations obtained during the tests the deformability of the flanged joint connecting the columns and of the box have been evaluated. The mechanical characteristics, assessed with the above experimental tests, have been used to build a simplified numerical model using both Strand7 (Strand 7 Pty Ltd., 2010) and OpenSees software (McKenna et al. 2007). Elastic beam elements with equivalent area and inertia have been used to model the columns and the steel support; elastic hinges have also been used to model the joints. The reference system (x,y,z) is indicated in Figure 1.

An eigenvalue analysis has been carried out to evaluate the natural frequencies of the switch, listed in Table 1 together with the prevailing direction of the modal displacement (T indicates a torsional mode round the z axis).

Table 1. Natural frequencies of the first five modes of vibration of the switch and relevant prevailing direction of the displacements

Mode N.	Frequency (Hz)	Direction
1	0.84	x
2	0.9	y
3	2.08	T
4	5.41	x
5	8.53	y

The evaluation of the seismic vulnerability of the circuit breaker cannot be performed according to a specific hazard condition because it is usually placed in different sites along the country. Consequently, the reference seismic action has been selected according to the AF5 spectrum provided by the CEI Standard (2008) that accounts for a peak ground acceleration (PGA) of 0.5g (see Figure 4).

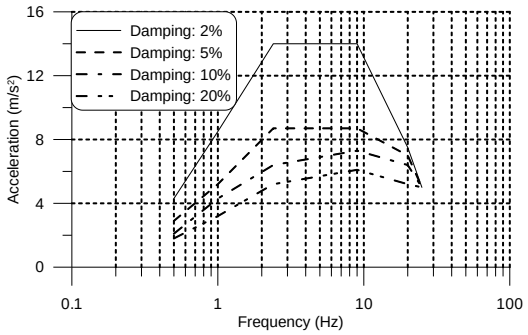

Figure 4. CEI Standard (2008) response spectra

By applying the AF5 spectrum (with 2% damping ratio, 100% in one direction and 30% in the orthogonal one), a maximum bending moment $M = 49.2kNm$ was obtained. This value is double than the ultimate value coming from the experimentally tests, which clearly demonstrate the inadequacy of the analysed apparatus in seismic prone-areas. Without further calculation, accounting for the AF5 spectrum as a median spectrum and without taking into account the dispersion in the ceramic strength, we can roughly conclude that the probability of collapse is about 50% for an event with intensity half of that given by the reference spectrum.

MODELING OF THE FORCE-DISPLACEMENT BEHAVIOUR OF THE WIRE-ROPES

Wire-Ropes are simply devices composed by steel wires spirally wrapped and blocked by two steel bars (see Figure 5). The response of these devices is substantially elastic and quasi-linear in both the horizontal directions but significantly non-linear in the vertical direction because of the variation in the geometry of the spires that widen in compression and tighten in tension. Consequently, the device shows a softening behaviour in compression and hardening behaviour in tension. During a cyclic action, friction between the wires produces significant energy dissipation.

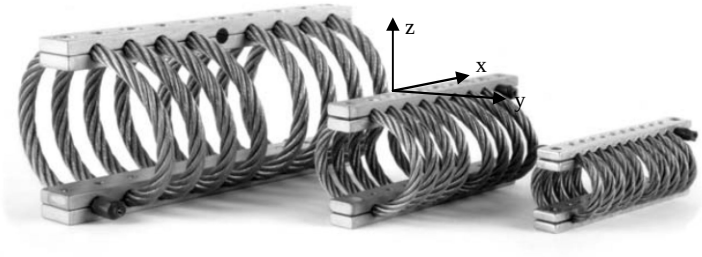

Figure 5. Wire-rope Devices

Figure 6 shows the experimental force-displacement cycles of a wire-rope along the principal directions: tension-compression (z), shear (x), roll (y) (Paolacci and Giannini 2008). They are obtained by applying the force along x, y and z, separately. Actually, the three responses are not independent because there is an interaction between the forces: compression reduces the shear and roll stiffness, while they are increased by tension. In the considered application, however, the shear forces are much smaller than the force in tension-compression; therefore the interaction has been neglected.

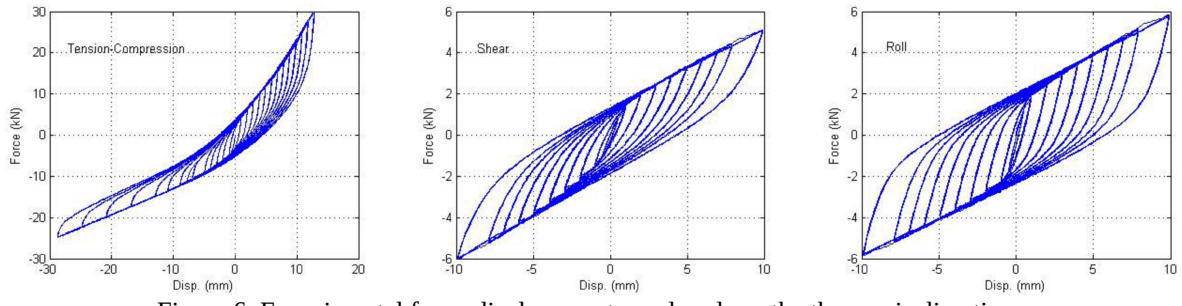

Figure 6. Experimental force-displacements cycles along the three axis directions

The shear and roll cycles can be easily modelled by the Bouc-Wen model (Wen, 1976); this is not true in tension-compression for which Bouc-Wen model shall be modified to represent the strong asymmetry in terms of force; some authors (Demetriades et al (1993)) have already formulated a modified version of the Bouc-Wen model. The constitutive equation generally used is the following:

$$F = f_1(x) + f_2(x)z \tag{1}$$

where $f_1(x)$ and $f_2(x)$ are functions of the displacement x; z is the internal variable of the Bouc-Wen law and it is the solution of the differential equation (2):

$$\dot{z} = A\left\{1 - \left[\beta sign(x\dot{z}) + \gamma\right]|z|^n\right\}\dot{x} \tag{2}$$

Equation (1) generalizes the formulation commonly used to model a symmetric hysteretic behaviour (Schwanen, (2004), Paolacci and Giannini (2008)):

$$F = Kx + F_0 z \tag{3}$$

where K is the asymptotic stiffness and z is the variable that describe the hysteretic law. In order to describe the tension-compression cycles of wire-ropes, the function $f_1(x)$ should account for the different asymptotic behaviour in tension and compression, while the function $f_2(x)$ should account for the different displacement amplitude of cycles, larger in tension than in compression. In this work, according to equation (1) a new formulation has been developed. By assuming that for $x > 0$ the stiffness tends to K_1, while for $x < 0$ the stiffness tends to K_2, it can be assumed:

$$\frac{df_1}{dx} = \frac{K_1 e^{x/x_0} + K_2 e^{-x/x_0}}{e^{x/x_0} + e^{-x/x_0}} \tag{4}$$

where x_0 is a parameter that modulates the rapidity of the transition from K_1 to K_2. By integrating the equation (4) we obtain:

$$f_1(x) = C + \left(\frac{K_1 - K_2}{2}\right) x_0 \, log\left(\frac{1 + e^{2x/x_0}}{2}\right) + K_2 x \tag{5}$$

Function $f_2(x)$ assumes generally an exponential form; in this work, the argument of the exponential is raised to a constant b that modulates the extent of variation of the cycle amplitude:

$$f_2(x) = F_0 \, exp\left[\left|\frac{x}{a}\right|^b sign(x)\right] \tag{6}$$

DESIGN AND MODELING OF THE BASE ISOLATION SYSTEM

The behaviour of the isolation system depends on two parameters that control the stiffness of the system: the axial stiffness of the wire-ropes and their position (distance from centre of the switch). Wire-rope isolators have been selected so that the natural frequencies of the isolated system was double of the non-isolated breaker. Accordingly, the device Enidine® WR28-400-08, made in Italy (on license) by the Powerflex® Company has been chosen. It is 150 mm long and is made with a cable of diameter ϕ 22mm. Two dispositions of the wire-ropes on a square steel foundation plate have been considered: one perpendicular to the diagonal of the square and one perpendicular to the medians; these will be indicate in the following with X and + respectively. In addition to the type WR28-400-08 other two types of wire-ropes have been considered: a more stiff (WR28-200-08) and a more flexible ones (WR28-800-08). Several configurations of the isolation device have been analyzed by varying the wire-rope typology and their distance from the centre of the steel plate.

A sample of 6 elements (2 for each isolator type) has been subjected to cyclic testing with variable amplitude in x, y and z direction (see Figure 6), aiming at identifying the parameter of the force-displacement law for each wire-rope. In shear and roll tests (along x and y), to account for the influence of the normal force on shear and roll deformability, a prestressing force has been applied

with several values. In fact, the tangential stiffness reduces with the increasing of the prestressing force, even though in the present case the tangential forces are one order of magnitude smaller than the normal force and the tangential deformability is therefore negligible. The identified parameters of the Wire-Rope type WR280-4 are reported in Table 2.

Table 2. Identified parameters for Tension-Compression, Shear and Roll behaviour of the Wire-Rope WR280-4

	Bouc-Wen			$f_1(x)$				$f_2(x)$		
	=	¥=	n	K_1 $\left(\frac{kN}{mm}\right)$	K_2 $\left(\frac{kN}{mm}\right)$	x_0 (mm)	C (kN)	F_0 (kN)	a (mm)	b
Shear	0.582	0.374	0.510	0.378	-	-	-	1.288	-	-
Roll	0.373	0.805	0.385	0.302	-	-	-	2.956	-	-
Tension-Comp.	1.425	-0.309	0.384	1.329	0.616	8.959	-0.588	0.190	26.919	0.751

An analytical model of isolated switch has been developed using the FE software OpenSEES (McKenna et al. 2007). The switch itself has been modelled as previously described, while the isolation device has been modelled with four triples of springs, representing the tension-compression, shear and roll behaviour respectively, connected to the switch by rigid elements that simulate the presence of the base plate. The model neglects the interaction between the three components of deformation. To model the constitutive laws of the springs in shear and roll, the Bouc-Wen model has been used with parameters calibrated on the results of the experimental tests executed with a prestressing force of $N = 6kN$, equal to the static load. To simulate the tension-compression behaviour a new element has been implemented into OpenSEES according to the modified Bouc-Wen model (equations (1), (5), (6)). Nine different configurations of the isolation systems have been analysed by varying type of wire-ropes and their distance from the centre of the plate. They are listed in Table 3.

Table 3. Configurations of the isolation system analyzed

Type	radius (mm)	N	Acronym
Fixed Base	-	0	FB
WR28-200	354	1	PX500
	424	2	PX600
WR28-400	300	3	M+600
	354	4	MX500
	389	5	MX550
	424	6	MX600
	537	7	MX700
WR28-800	380	8	G+760
	537	9	GX760

Non-linear dynamic analysis have been performed by using 9 triple of accelerograms selected from the PEER Database. The records have been chosen among those generated by earthquakes with magnitude from 5 to 7 and distance source-site from 5 to 30 km. No specific soil type has been considered because of the vagueness of the location. Among these records 9 triples have been selected so that the mean spectrum of each component matched as best as possible the CEI spectrum with a peak ground acceleration (PGA) of 0.5g and 2% damping. They are listed in Table 4 whose response spectra are shown in Figure 7. The CEI spectrum does not take into account the vertical component; consequently, the EC8 (EN1998-1:2005) spectrum has been considered for this purpose.

In order to fit better the target spectra, the records have been modified by SeismoMatch software (2013); they have been modified both in amplitude and frequency preserving some of the characteristics of the natural records such as the non-stationarity.

Table 4. Selected records

Event number	Event	Station	Year	Magnitude	Dist. (kM)	Mechanism
NGA 721	Superstition Hills-02	El Centro Imp. Co. Cent.	1987	6.54	18.2	Strike-Slip
NGA 767	Loma Prieta	Gilroy Array #3	1989	6.93	12.2	Reverse-Oblique
NGA 778	Loma Prieta	Hollister Diff. Array	1989	6.93	24.5	Reverse-Oblique
NGA 802	Loma Prieta	Saratoga – Aloha Ave	1989	6.93	7.60	Reverse-Oblique
NGA 1077	Northridge-01	Santa Monica City Hall	1994	6.69	17.3	Reverse
NGA 2374	Chi-Chi, Taiwan-04	CHY074	1999	6.20	6.00	Strike-Slip
NGA 1111	Kobe, Japan	Nishi-Akashi	1995	6.90	7.10	Strike-Slip
NGA 729	Superstition Hills-02	Wild Liquef. Array	1987	6.54	23.9	Strike-Slip
NGA 752	Loma Prieta	Capitola	1989	6.93	8.70	Reverse-Oblique

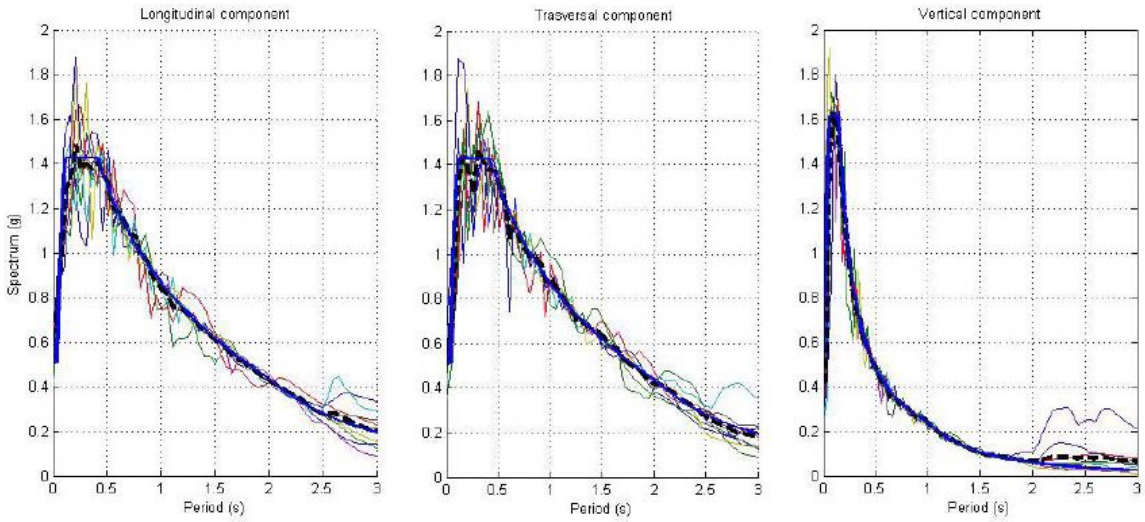

Figure 7. Response spectra of the nine selected accelerograms and relevant mean spectrum (dashed line) afetr matching to the reference spectrum (solid line)

A synthesis of the results of the non-linear dynamic analysis are shown in Figure 8 and Figure 9. Figure 8 shows the maximum bending moments at the base section of ceramic column (the most critical section of the structure); these results, are compared to the results obtained for the non-isolated system.

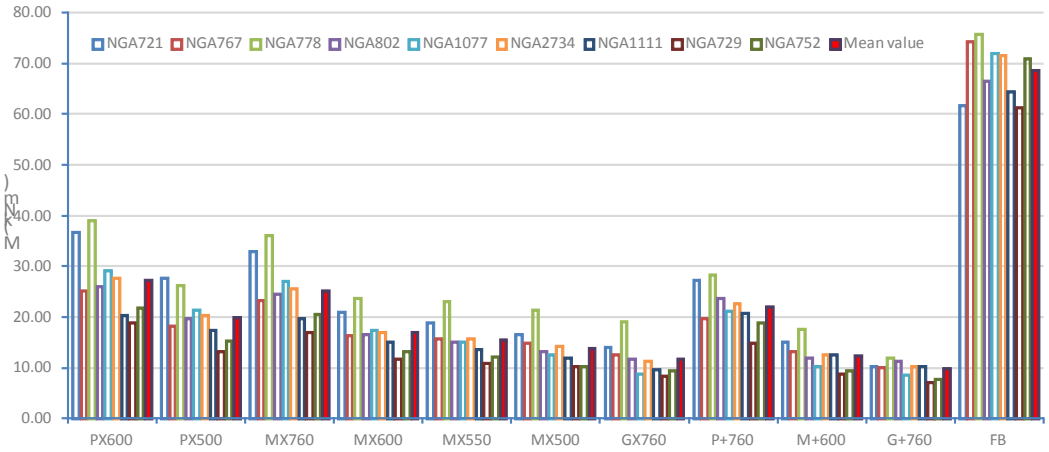

Figure 8. Maximum Bending moment at the base section of the ceramic column

The Figure 9 shows the maximum displacements in the longitudinal direction. In this case, the values are compared with the value obtained by applying statically the wind force. The comparison

between the bending moment of isolated and non-isolated system points out the effectiveness of the isolation devices in all the considered configurations. Comparing the maximum displacements, it can be noticed that the seismic displacement is not very sensitive to the system configuration (the periods of vibration of the system is larger than 2sec.), while the wind displacements is conditioned to the flexibility of the wire-ropes. This shall be taken into account in the choice of the better configuration. This consideration leads to the exclusion of the more flexible isolators (configuration GX760, M+600, G+760 in table 3). A very large displacement, in fact, causes a displacement of the cables that connect the switch with the adjacent equipment, which may be unacceptable for the electrical insulation conditions of the conductors. The configuration that best meet all the requirements seems to be the MX500, characterized by wire-ropes WR28-400 placed at a distance r = 354 mm from the centre and orthogonal to the diagonals of the square plate. With this configuration the mean value of the bending moment is $\bar{M} = 13.9 kNm$ and the displacement caused by the wind is $S_{wx} = 120 mm$.

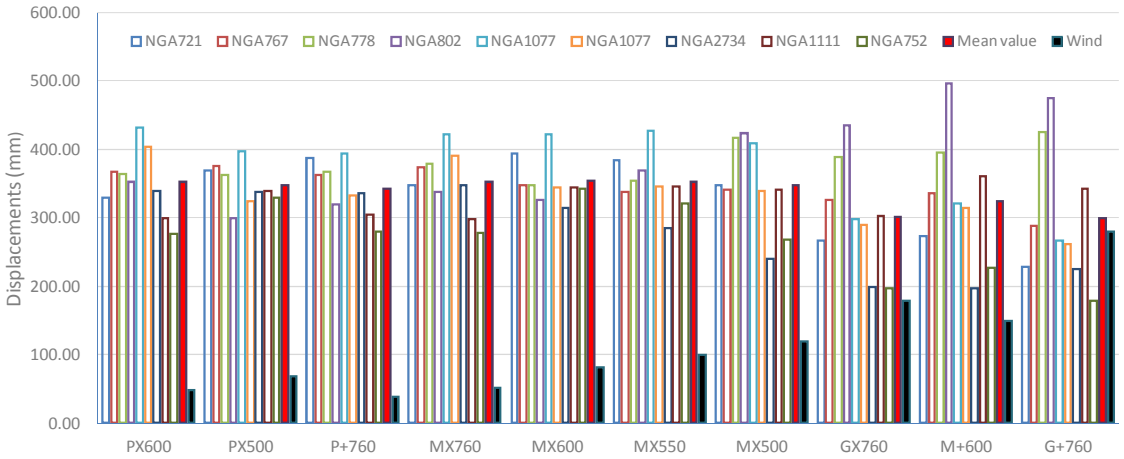

Figure 9. Maximum displacements in the longitudinal direction

SHAKING TABLE TEST CAMPAING

The results obtained numerically have been validated through a series of shaking table tests both for isolated and non-isolated configurations. Two isolation system configurations have been tested, both equipped with wire-ropes type PWHS2200508M2 produced by Powerflex (corresponding the type WR28-200 Enidine): X500 and +380. In the original configuration the capacitors were placed on the same side of the operating cabinet; consequently a gravity loads eccentricity caused an asymmetric vertical deformation of the wire-ropes, resulting in a pronounced inclination of the switch. To overcome this drawback, the position of the capacitors was reversed.

The instrumentation used for the tests executed on the non-isolated circuit breaker was composed by: 13 accelerometers placed on the breaker (placed at the ceramic column base, at the flanged joint and at the end of the chambers), 3 accelerometers on the shaking table, 10 strain-gauges and 1 linear transducer (to measure the absolute displacement at the top of the switch along the longitudinal direction). 14 displacements transducers have been added for the tests on the isolated structure.

Sine-sweep analyses with small intensity (0.01g) have been carried out on the non-isolated switch to identify its natural vibration frequencies and the corresponding modal shapes. Experimental tests results have been compared with those obtained analytically. To improve the agreement, the mechanical properties of the elastic hinges, used to model the flanged joints and the metallic box, were adjusted, given the uncertainty of their stiffness. In Table 5 the experimental vibration frequencies of the first five modes are listed together to the corresponding direction and damping. In the same table they are compared with the analytical ones, including a numerical reproduction of the sine-sweep test. The analytical results are coincident while a slight difference remains with the experimental ones.

Table 5. Comparison between experimental-analytical frequencies (Hz), prevailing direction of the displacements and measured damping of the first vibration modes

	Mode	1	2	3	4	5
Experimental	Direction	*x*	*y*	*T*	*x*	*y*
	Damping (%)	3.3	3.9	2.8	1.3	1.0
	Frequency (Hz)	0.96	0.98	2.19	5.62	9.6
Numerical Frequencies(Hz)	Modal Analysis	0.94	1.02	2.08	5.53	8.77
	Sine Sweep	0.94	1.02	-	5.53	8.76

Figure 10 shows the comparison between the experimental modal shapes of modes 1 and 4 (in the x direction) and modes 2 and 5 (in the z direction) together with those obtained analytically by modal analysis and the simulation of the sine-sweep test. The results are in good agreement.

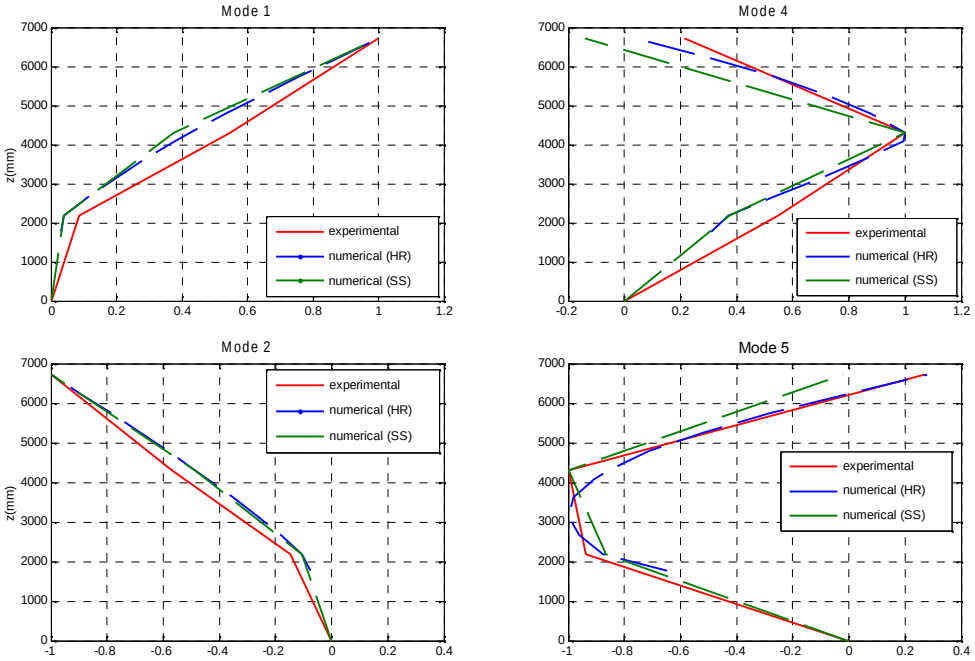

Figure 10. Comparison between experimental and analytical modal shapes of the switch

After the dynamic characterisation, the apparatus was base isolated and subjected to sine-sweep signals and 6 accelerograms; in particular, 3 of the nine triples of accelerograms used for the analysis and 3 other signals artificially generated.

In the selection of the input signals the maximum allowable displacement of the shaking table ($\pm 100mm$) was taken into account by applying a high pass filter to the records. Accordingly, a subset of the accelerograms of table 3 have been selected: NGA 729, NGA 752, NGA 1111.

In addition, artificial records have also been generated by the software SIMQKE (Gasparini and Vanmarcke, 1976). A better matching of the response spectra with the reference response spectrum has been obtained, even though they are less realistic. In addition, the artificial records have been filtered to reduce the maximum displacement. Despite of these precautions, only two records allowed to reach the maximum foreseen intensity (PGA = 0.5g). The dynamic tests have been performed by scaling gradually the records starting from the 25%-30% of the intensity up to the maximum value imposed by the table limit (71%, 100%). The most significant measurements have been compared with those obtained analytically. The experimental displacements along the breaker have been evaluated by integrating the acceleration signals.

Figure 11 shows the analytical-experimental comparison between the horizontal top displacements obtained for the accelerogram A729 whereby the maximum value of the intensity has been reached. The analytical displacements show a good agreement with the experimental results, except for the peak displacements.

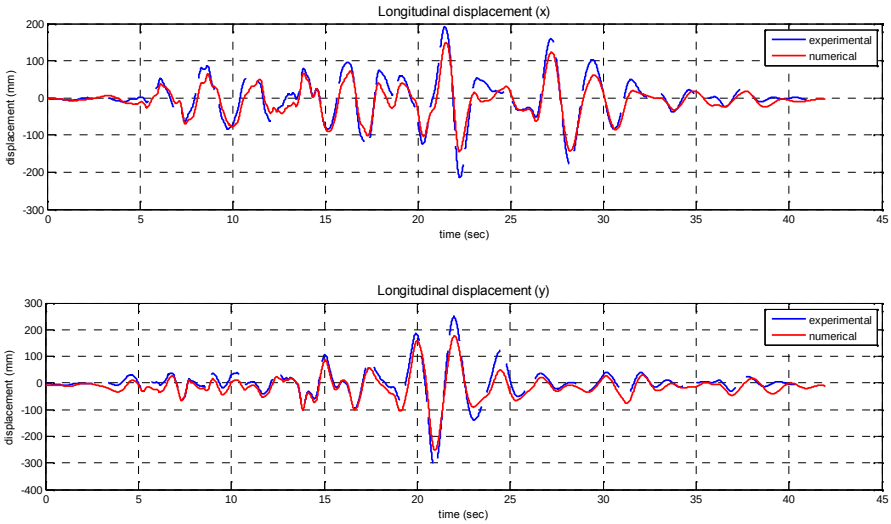

Figure 11. Analytical-numercial comparison: top displacements in x and y direction – A729

The same difference was observed for all tests. A good agreement was also observed comparing the bending moment at the column base and the vertical displacements of the wire-ropes (Figure 12, 13).

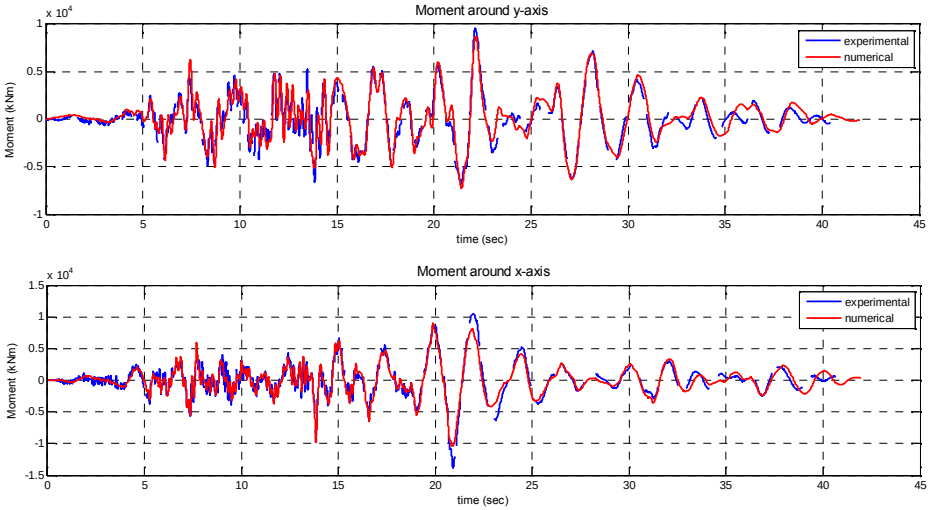

Figure 12 – Analytical-numercial comparison: bending moment at ceramic column base in x and y direction – Isolators in X500 configuration – accelerogram A729 (100%)

Because of the displacement limits of the shaking table, the base isolated circuit breaker did not collapse during the foreseen tests. Consequently, it was decided to test the non-isolated breaker in collapse conditions using one of the artificially generated accelerograms (ART3), one of the artificial for which it was possible to reach the maximum intensity). This latter has been used for a better matching with the reference spectrum.

The tests have been performed by scaling the record at 25%, 30% and 50% until the collapse was reached, which corresponds to an ultimate bending moment $M = 22kNm$. This value is smaller than that ultimate moment reached during the cyclic tests. This difference is probably due to the test mode not to the mechanical characteristics of the column, given that the same ultimate moment was reached for all specimens during the cyclic tests.

Some sine-sweep tests in the longitudinal direction tests have also been performed for the characterisation of the non-isolated apparatus in aftershock conditions. The natural frequency of the first mode reduced from 0.96Hz to 0.91Hz, showing a reduction in the stiffness that should be attributable to the flanged joints.

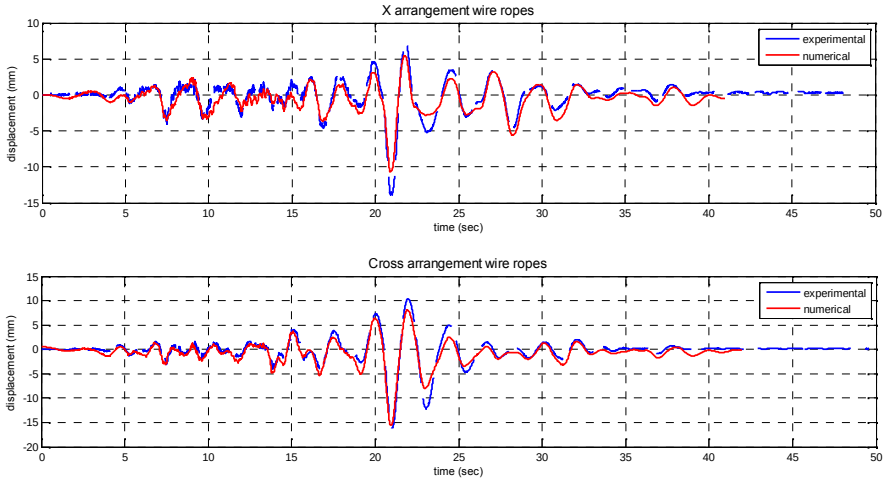

Figure 13 – Analytical-numercial comparison: Vertical displacements in the wire-ropes for isolated Beraker with configurations X500 and + 380– accelerogram A729

Figure 14 shows the moment-rotation cycles of the joints obtained at different times during the experimental campaign (first tests, first test after changing the disposition or the wire-ropes from X to +, last test on the isolated switch). The straight lines represent the tendency of the cycles whose slope can be considered as an elastic stiffness approximating the real cycle. A reduction of the stiffness and a sensible loss of linearity (highlighted by hysteresis) is shown particularly in the intermediate joint. The measures of the stiffness have bees used to modify the numerical model.

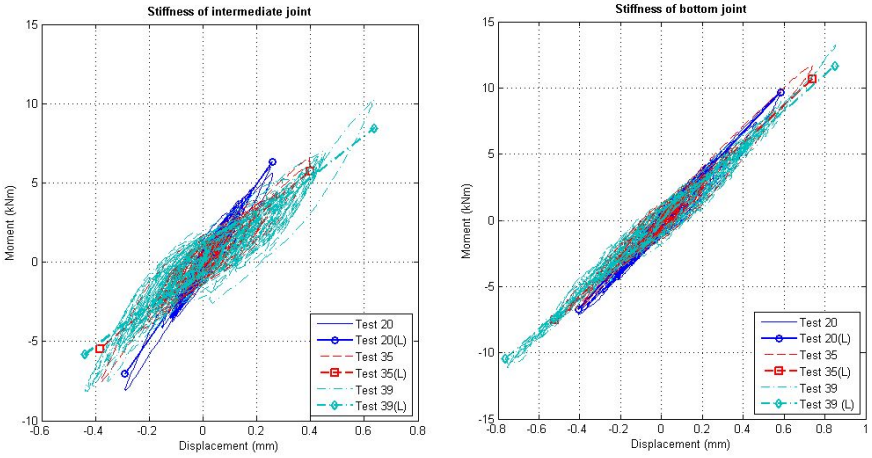

Figure 14. Experimental moment-rotation cycles of the joints

CONCLUSIONS

The sismic vulnerability of some old components of HV electrical power network substations, and more in particular of circuit breakers, has been shown by recent eartquake. For this reason the italian Transmission System Operator (TERNA) has established an agreement with the University of Roma Tre to design a new base isolation system of circuit breakers.

The proposed solution is based on steel cable dampers already know as wire-ropes elements. Wire-ropes devices can work in rocking and then in tension-compression, differently from the devices usually employed for the base isolation of civil and industrial structures that work in shear. As consequence, the elongation of the natural vibration period of the structure and the increasing of the damping ratio due to the friction between wires are obtained. Consequently, the stress level in the

structure is drastically reduced. Several configurations have been analyzed, by varying type and disposition of the isolation devices. The selection of a proper devices typology is a compromise between the reduction of the stress in the structure and the limitation of displacements caused by the wind. In fact, this latter can cause incompatibility of the isolation system with the electrical insulation conditions due to the movement of the electrical cable connected to the circuit breaker. In order to complete the investigation and to validate the results obtained numerically, a shaking table test campaign has been performed both for the isolated and non-isolated circuit breaker. The results have shown both the effectiveness of the new isolation system and the reliability of the proposed FE model. A picture of the installation is showed in Figure 15.

Figure 15. Installation of the seismic isolation system

REFERENCES

CEI EN 62271-207 (2008). High-voltage switchgear and controlgear Part 207: Seismic qualification for gas insulated switchgear assemblies for rated voltages above 52 kV.

Demetriades G.F., Constantinou M.C., Reinhorn, A.M. (1993). “Study of wire rope systems for seismic protection of equipment in buildings”. Engineering structures, 15:321-334.

Di Donna, M., Serino, G., Giannini, R. (2002). Advance earthquake protection systems for high voltage electric equipment, 12th European Conference on Earthquake Engineering, London, September.

EN1998-1:2005. Design of Structures for Earthquake Resistance Part 1: General Rules, Seismic Actions and Rules for Buildings. Comitè e Europaèen de Normalisation: Brussels, 2005.

Knight, B. and Kempner, Jr., L. (2009) Seismic Vulnerabilities and Retrofit of High-Voltage Electrical Substation Facilities. TCLEE 2009: pp. 1-12.

Kong, D. and Reinhorn, A. (2009) Seismic Evaluation and Protection of High Voltage Disconnect Switches. TCLEE 2009: pp. 1-11.

Gasparini, D. and Vanmarcke, E. H. (1976) SIMQKE: A Program for Artificial Motion Generation, Department of Civil Engineering, Massachusetts Institute of Technology, Cambridge, MA.

McKenna F, Fenves GL, Scott MH. (2007). OpenSees: open system for earthquake engineering simulation. PEER, University of California: Berkeley, CA, 2007.

Paolacci F., Giannini R. (2008). “Study of the effectiveness of steel cable dampers for the seismic protection of electrical equipment”. In Proceedings of The 14th World Conference on Earthquake Engineering, Beijing, China, October.

PEER Strong Motion Database. Pacific Earthquake Engineering Research. Available from: http://peer.berkeley.edu/smcat/ [Accessed on January 2012].

Schwanen W. (2004). Modelling and identification of the dynamic behavior of a wire rope spring. Technische Universiteit Eindhoven, The Netherlands, Report number: DCT-2004/28, Master Thesis, 2004

Seismosoft (2013). "SeismoMatch v2.1 – A computer program for spectrum matching of earthquake records," available from http://www.seismosoft.com.

Wen, Y. (1976). Method for random vibration of hysteretic systems. Journal of the Engineering Mechanical Division, Proceeding ASCE, 102:2, 249-263